Supporting Information

Nanotubular Fe_2O_3 and Mn_3O_4 with hierarchical porosity as high-performance anode materials for lithium-ion batteries

Zhen Li[a*], Man Yang[a,b], Fengting Geng[a,c], Dashuai Zhang[a], Yongzheng Zhang[a], Xiuling Zhang[a], Xuliang Pang[a*], Longlong Geng[a,b,c*]

[a]Shandong Provincial Key Laboratory of Monocrystalline Silicon Semiconductor Materials and Technology, College of Chemistry and Chemical Engineering, Dezhou University, Dezhou 253023, P. R. China

[b]School of Chemical Engineering and Technology, North University of China, Taiyuan 030051, PR China

[c]School of Chemistry and Chemical Engineering, Shandong University of Technology, Zibo 255000, PR China

*Email: lizhendiyi@163.com (Zhen Li); pangxuliang163@163.com (Xuliang Pang); llgeng@126.com (Longlong Geng)

Materials Characterization

Powdery X-ray diffraction (XRD) analysis was conducted on a BRUKER D2 PHASER X-Ray Diffractometer with Cu Kα radiation. The microstructure and morphology of the materials were characterized by a field-emission scanning electron microscopy (FE-SEM, Hitachi S4800) and transmission electron microscopy (Hitachi H-800 TEM at 200 kV). The chemical state of the materials was analyzed by X-ray photoelectron spectroscopy (XPS, Thermo ESCALAB 250XI equipped with an Al Kα X-ray source). The N_2 adsorption-desorption isotherms were obtained using a Micromeritics ASAP

2460 at 77 K. The specific surface area and porosity were calculated by using Brunauer-Emmett-Teller (BET) and Barrett-Joyner-Halenda (BJH) models, respectively. Thermogravimetric analysis (TGA) was performed in air within the temperature range from 25 to 800 °C (TA Instruments Hi-Res TGA 2950).

Electrochemical measurements

The active materials, conductive material (Super P), and binder (polyvinylidene fluoride, PVDF) in a weight ratio of 7:2:1 was dispersed into N-methyl pyrrolidone (NMP) to form a stable slurry. The working electrode was prepared by coating the slurry of onto a round-shaped copper foil (1.1 cm^2). The density of the active material is about 1.3 mg cm^{-2}. The electrochemical performance of the as-fabricated working electrodes was examined using LIR2032 coin-type half cells with 1 M LiPF6 in a mixture of ethylene carbonate (EC), dimethylcarbonate (DMC) and diethylcarbonate (DEC) (1: 1: 1, v/v/v) as the electrolyte. Lithium foil was used as both the counter electrode and the reference electrode. The electrochemical performance of the working electrodes was tested by using a battery test system (NEWARE CT-3008 W). The potential window for the anode is within the range of 0.01-3.0 V vs. Li/Li^+, while for the $LiMn_2O_4$ cathode is ranging from 3.3 to 4.4 V. Electrochemical impedance spectra (EIS) were collected for the fresh cells at an open potential over the frequency range from 100 kHz to 0.01 Hz on an electrochemical workstation (Shanghai Chen Hua CHI660D). Cyclic voltammetry (CV) was performed on the anodes at various scan rate ranging from 0.1 to 0.8 mV s^{-1} within the potential window of 0.01–3.0 V. The charge/discharge measurements at 50 mA g^{-1} for the coin-type Fe_2O_3-based full cell were performed within the voltage range of 1.4 -3.5 V, while it was carried out within the potential window of 2.0-4.2 V for the Mn_3O_4-based full cell.

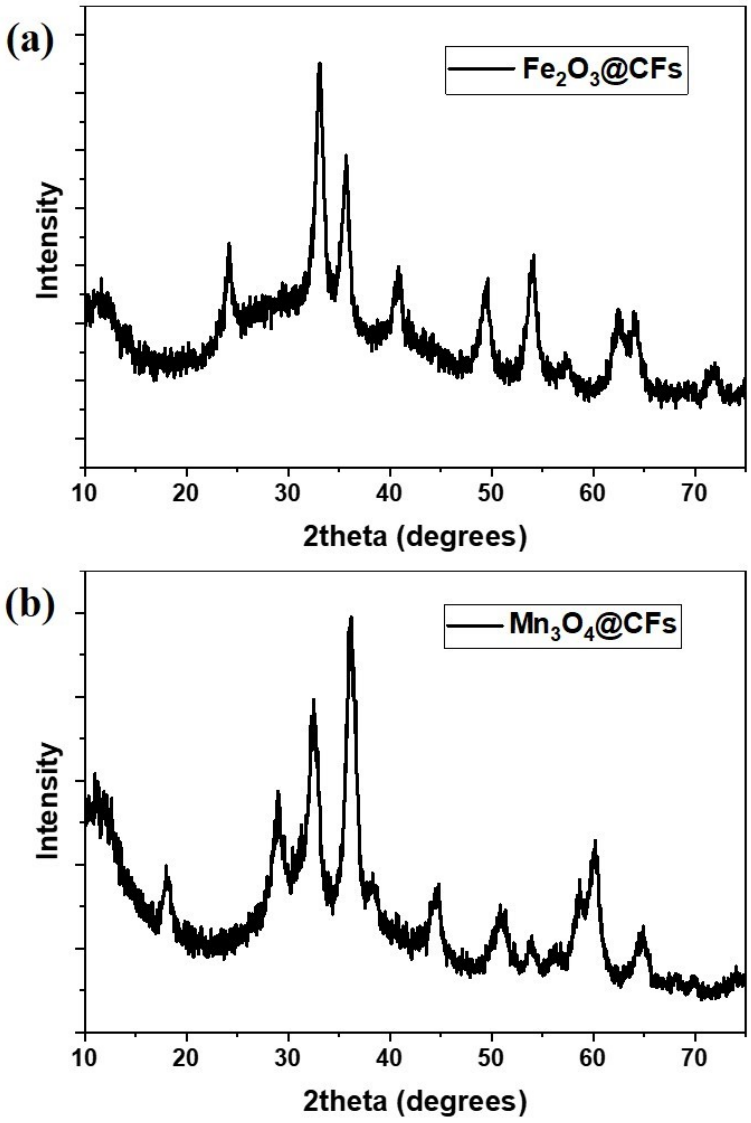

Fig. S1 PXRD patterns of M_xO_y@CFs

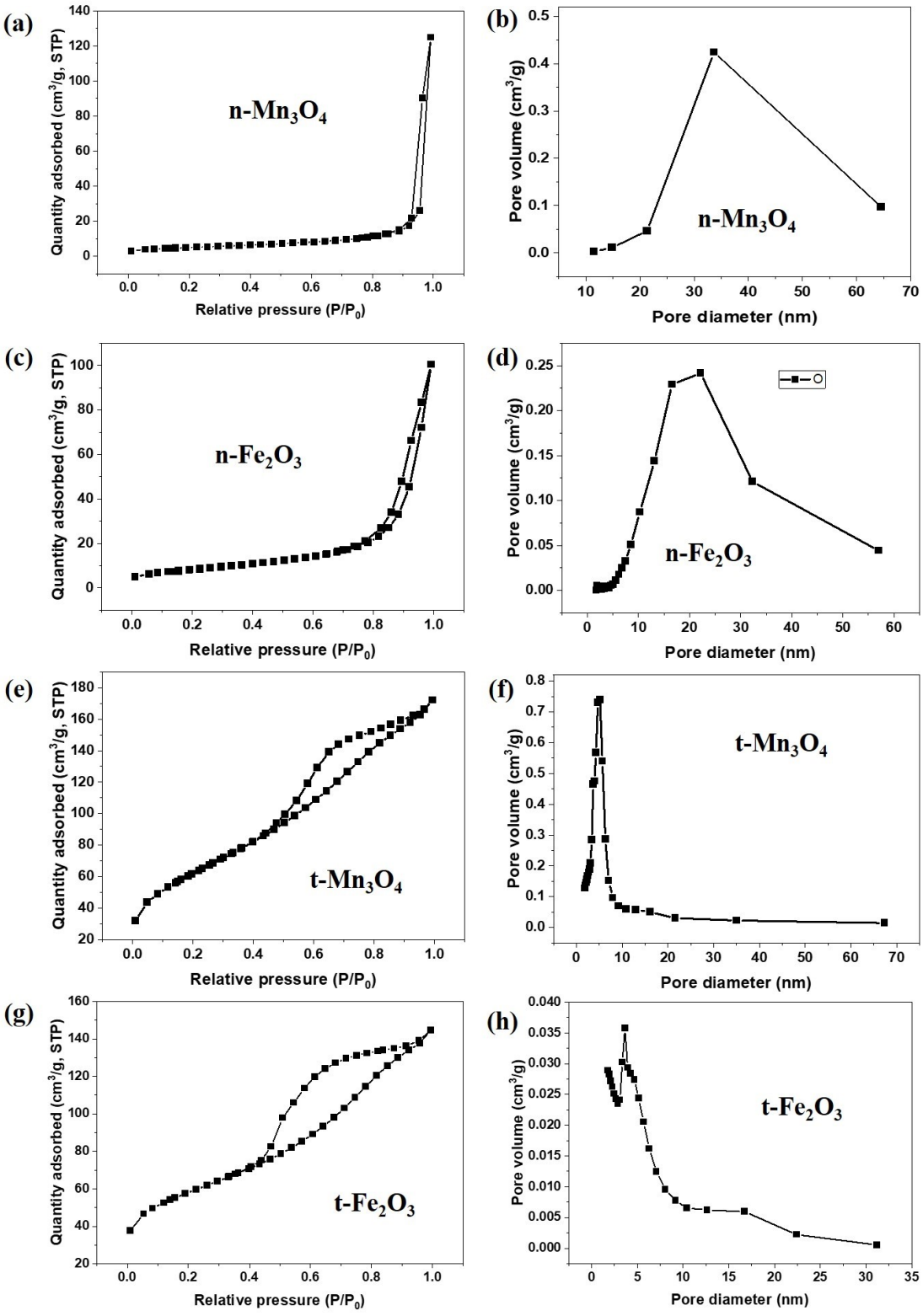

Fig. S2 N_2 adsorption–desorption isotherms of the materials and the corresponding pore size distributions calculated from the desorption curves by the BJH method.

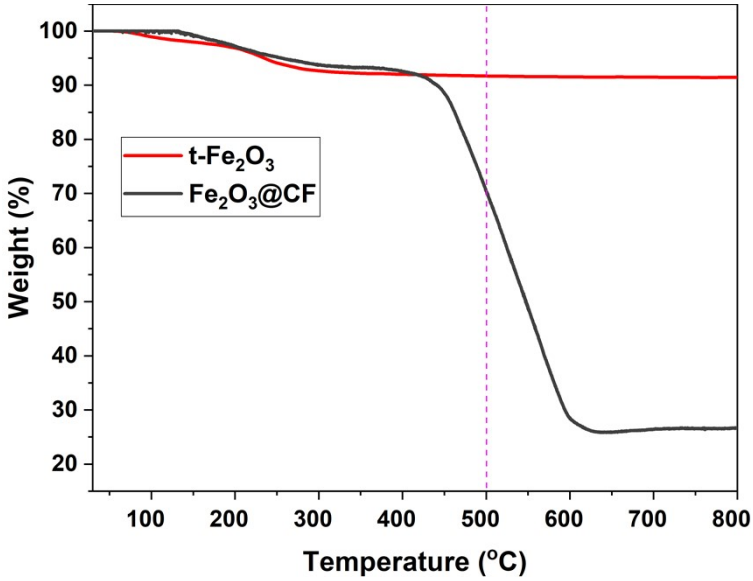

Fig. S3 TGA curves of Fe_2O_3-based materials

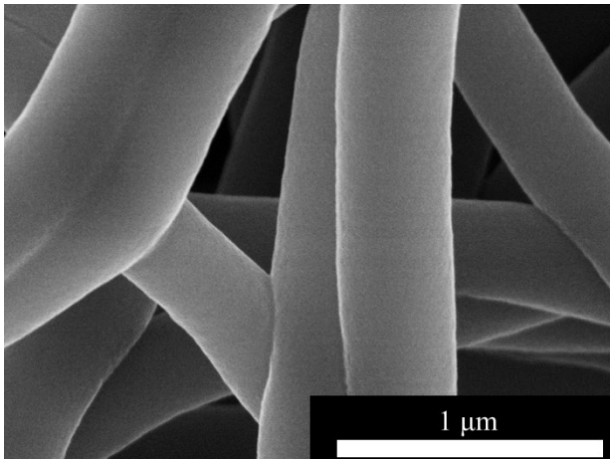

Fig. S4 FE-SEM imagine of CFs.

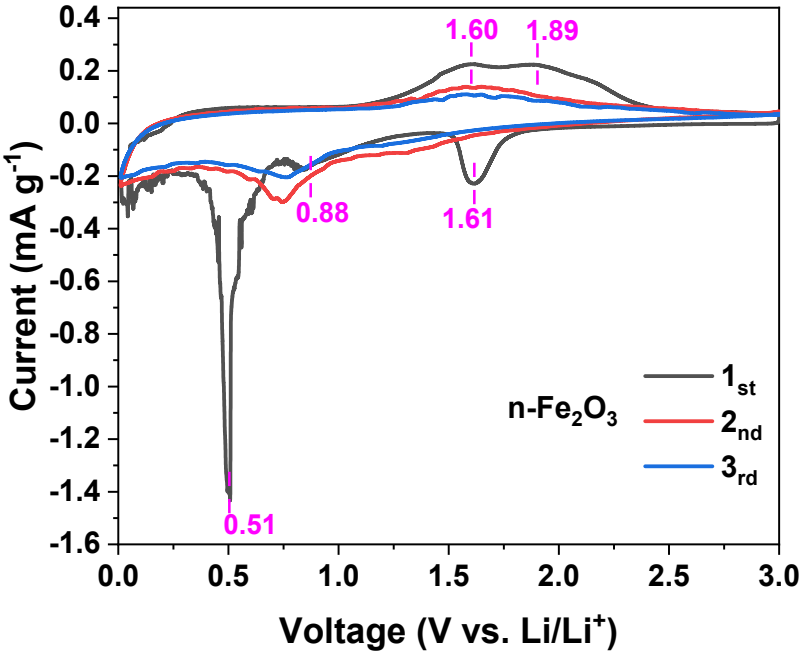

Fig. S5 The first 3 CV cycles of the n-Fe_2O_3 electrode

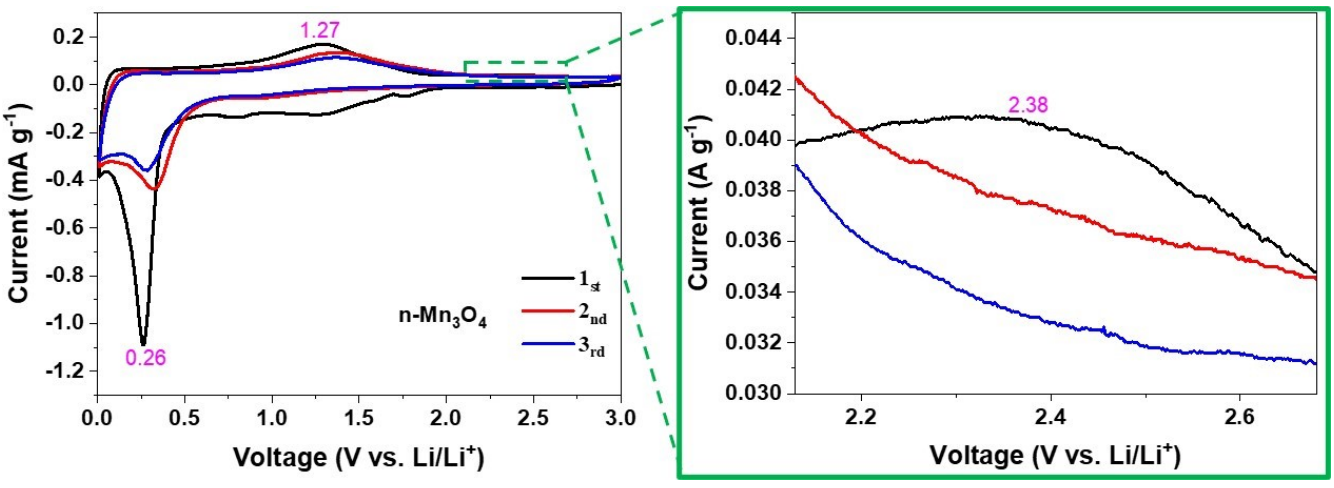

Fig. S6 The first 3 CV cycles of the n-Mn_3O_4 electrode with the magnification within the voltage range of 2.15-2.65 V.

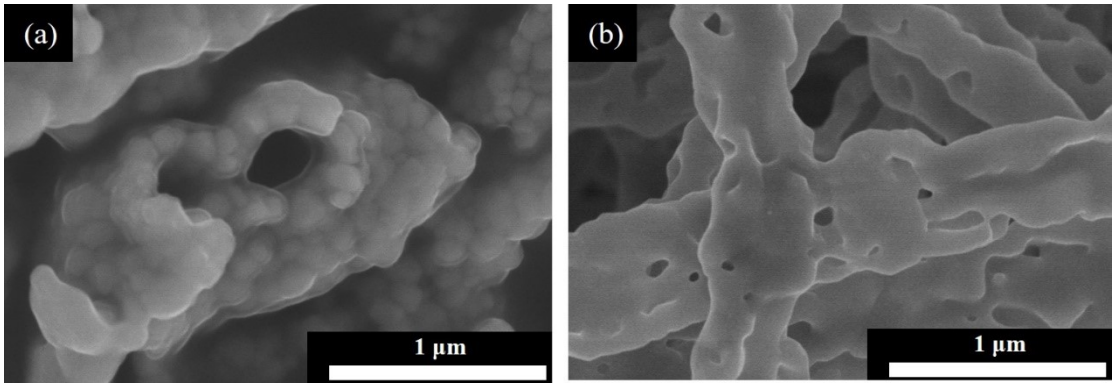

Fig. S7 FE-SEM images for the cycled t-Fe_2O_3 (a) and t-Mn_3O_4 (b) electrodes

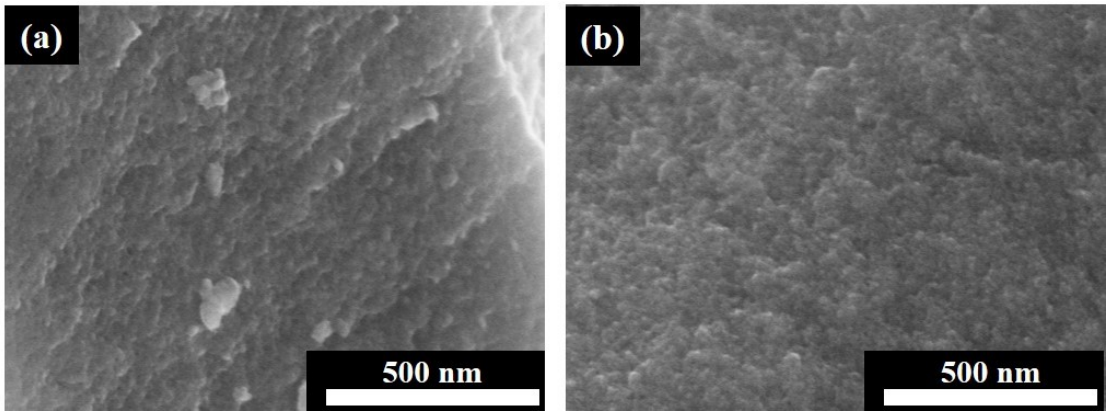

Fig. S8 FE-SEM images for the cycled n-Fe_2O_3 (a) and n-Mn_3O_4 (b) electrodes

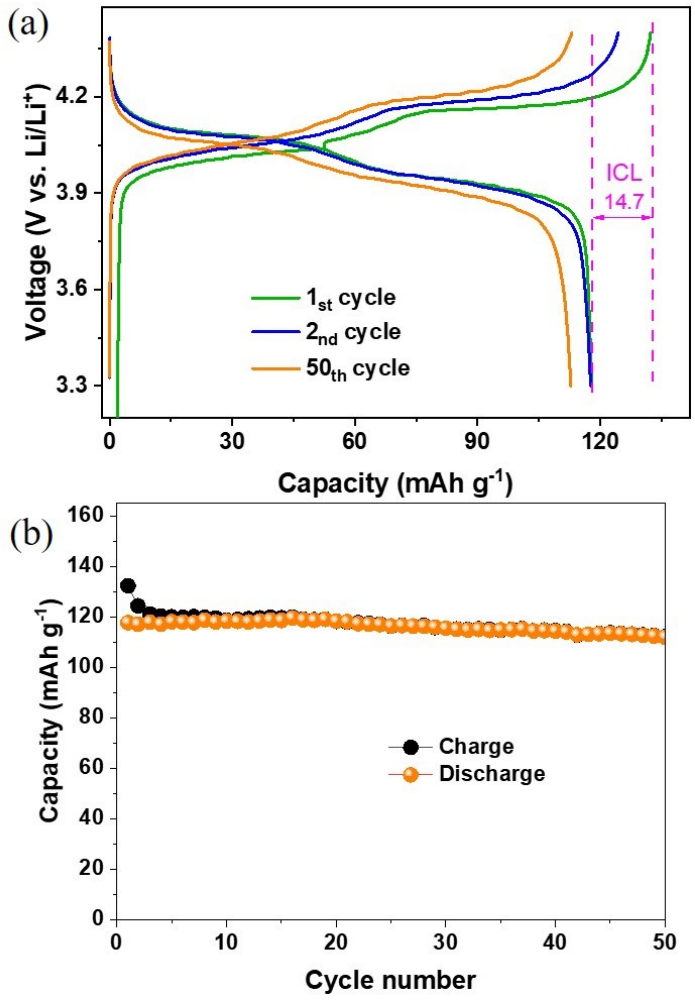

Fig. S9 Charge/discharge curves at different cycling states within the potential window of 3.3-4.4 V (a) and the cycling stability of the $LiMn_2O_4$ cathode (b)

Table S1 Comparison of electrochemical performance between different materials

Materials	Specific capacity (mAh g^{-1})	Ref.
t-Fe_2O_3	859.7 at 50 mA g^{-1}	**This work**
t-Mn_3O_4	901.4 at 50 mA g^{-1}	
Fe_2O_3@Fe_3O_4@$FeCO_3$/ reduced graphene oxide	868.7 at 200 mA g^{-1}	Appl surf. Sci., 2022, 605, 154798
MIL-88B(Fe) MOF	486 at 100 mA g^{-1}	Electrochim. Acta, 2023, 465, 142989
MIL-53(Fe)@RGO	550 at 100 mA g^{-1}	Electrochim. Acta, 2017, 246, 528–535
rGO/Mn_3O_4 nanocomposite	795.5 mAh g^{-1} at 100 mA g^{-1}	Ceram. Int., 2022, 21, 31923-31930
Mn-TBI coordination polymer	525 at 50 mA g^{-1}	Cryst. Growth Des. 2019, 19, 6503–6510
MnO@C composites	1221 at 100 mA g^{-1}.	Nanoscale, 2015,7, 9637-9645
PA-TA COF	543 at 1.0 A·g^{-1}	Nano Res., 2022, 15, 9779–9784
DAB-NiPc COF	941 at 100 mA g^{-1}	Chem. Eng. J. 2021, 425, 131630